P12.166 MODELING RADAR POWER AND PHASE ANTENNA PATTERNS AND THE EVALUATION OF DUAL-POLARIZATION ANTENNA PERFORMANCE

J.C. Hubbert[1]* and R.Rilling

National Center for Atmospheric Research, Boulder, CO

1. INTRODUCTION

Many radars are adopting the simultaneous transmission of horizontal (H) and vertical (V) polarized waves in order to achieve dual polarization measurements. Cross-coupling of the H and V waves can bias the dual polarization measurements (Hubbert et al. 2010a,b). Antenna polarization errors are one cause of such cross-coupling and it is desirable to minimize the antenna polarization errors. One figure of merit for performance of an antenna is ICPR (Integrated Cross-Polarization Ratio) defined as the LDR (Linear Depolarization Ratio) when the radar beam is filled with small spherical scatterers (Chandrasekar and Keeler 1993). Typically, only antenna power patterns are available and the phase patterns are unknown, especially for crosspolar antenna patterns. Thus, the upper bound of ICPR (ICPR$_{ub}$) is evaluated from the antenna power patterns. It is now possible to accurately model the complex antenna patterns if the antenna reflector surface can be measured and the antenna pattern of the feedhorn is known. In this paper the performance of the S-Pol (NCAR's S-band polarimetric radar) antenna is evaluated using a GRASP (General Reflector Antenna Software Package) software.

2. ANTENNA MODELING

In order to accurately assess and predict the antenna patterns of the S-Pol antenna, the shape of the surface of the parabolic reflector needs to be measured. One way to do this is via photogrammetry. Figure 1 (top panel) shows the S-Pol reflector with about 1400 optical patches applied (darker spots). The bottom panel of Fig. 1 shows the S-Pol dish at night using flash photography. The optical patches reflect light back toward the light source regardless of incident angle. By taking about 100 pictures of the dish at various location around it perimeter, the location of the optical patches can be determined in reference to a coordinate system. The uncertainty of the measurements are 0.001 in. to 0.002 in. A best fit parabola can be determined and the RMS error of the surface of the dish was found to be 0.033in. The focal length is 150.3 in. To model the complete antenna, support strut and feedhorn blockage is included. The antenna pattern of the feedhorn is the input. The output is the far-field pattern of the complete antenna system.

3. THEORETICAL ICPR

The complex antenna patterns are put into matrix form for the *transmitted wave* as

$$F = \begin{bmatrix} f_{hh} & f_{vh} \\ f_{hv} & f_{vv} \end{bmatrix} \quad (1)$$

where f_{hh}, f_{vh} are the complex copolar and crosspolar patterns for transmit H and f_{vv}, f_{hv} the complex copolar and crosspolar patterns for transmit V (Chandrasekar and Keeler 1993). Then the received voltages for a single spherical scatterer are,

$$\begin{bmatrix} V_h \\ V_v \end{bmatrix} = \begin{bmatrix} f_{hh} & f_{hv} \\ f_{vh} & f_{vv} \end{bmatrix} I \begin{bmatrix} f_{hh} & f_{vh} \\ f_{hv} & f_{vv} \end{bmatrix} \begin{bmatrix} E_h \\ E_v \end{bmatrix} \quad (2)$$

Expanding gives,

$$\begin{bmatrix} V_h \\ V_v \end{bmatrix} = \begin{bmatrix} f_{hh}^2 + f_{hv}^2 & f_{hh}f_{vh} + f_{vv}f_{hv} \\ f_{hh}f_{vh} + f_{vv}f_{hv} & f_{vv}^2 + f_{vh}^2 \end{bmatrix} \begin{bmatrix} E_h \\ E_v \end{bmatrix} \quad (3)$$

where I is the identity matrix representing a single spherical scatter.

System limit LDR (i.e., all scatterers in the radar resolution volume are spherical) is expressed ($E_h = 1$, $E_v = 0$) for a collection of spherical scatterers,

$$ICPR = LDR_{limit} = 10\log_{10}\frac{|V_v|^2}{|V_h|^2} = 10\log_{10}\frac{\sum_i |(f_{hh}f_{vh} + f_{vv}f_{hv})|^2 \sin\theta\delta\theta\delta\phi}{\sum_i (|f_{hh}^2 + f_{hv}^2|)^2 \sin\theta\delta\theta\delta\phi} \quad (4)$$

where i, the index over the antenna patterns, is understood. Integration over the random collection of spherical scatterers can be separated from the summation over

*NCAR/EOL, Boulder, Colorado 80307, email: hubbert@ucar.edu

the antenna patterns (see Wang and Chandrasekar (2006) for details). The effect of of the random distribution of particles in the antenna pattern is important to understand in terms of the form of Eq.(4). For a particular angle of θ and ϕ (indicated by the subscript i in Eq.(4)), the sum of $f_{hh}(i)f_{vh}(i) + f_{vv}(i)f_{hv}(i)$ is coherent (i.e., addition of complex numbers); however, the sum over two distinct angles, say i and $i+m$, is *incoherent*, i.e., the powers are added, $|f_{hh}(i)f_{vh}(i) + f_{vv}(i)f_{hv}(i)|^2 + |f_{hh}(i+m)f_{vh}(i+m) + f_{vv}(i+m)f_{hv}(i+m)|^2$. Executing the magnitude square operation in Eq.(4) gives:

$$ICPR = 10\log_{10}\Big[\frac{\sum_i[|f_{hh}|^2|f_{vh}|^2 + |f_{vv}|^2|f_{hv}|^2 + 2\Re(f_{hh}f_{vv}^*f_{vh}f_{hv}^*)]\sin\theta\delta\theta\delta\phi}{\sum_i|(f_{hh}^2 + f_{hv}^2)|^2\sin\theta\delta\theta\delta\phi}\Big] \tag{5}$$

Then the ICPR upper bound is

$$ICPR_{ub} = 10\log_{10}\frac{\sum_i[|f_{hh}|^2|f_{hv}|^2 + |f_{vv}|^2|f_{vh}|^2 + 2(|f_{hh}||f_{vv}||f_{vh}||f_{hv}|)]\sin\theta\delta\theta\delta\phi}{|(|f_{hh}|^2 - |f_{hv}|^2)|^2\sin\theta\delta\theta\delta\phi} \tag{6}$$

using the triangle inequality in the denominator.

4. MODELING RESULTS

From measurements in light rain, the ICPR of the S-Pol radar is about -31 dB and it is desired to lower that figure. The model is used to generate antenna patterns for the distorted dish and for blockage due to the feedhorn and support struts. The struts are modeled both with the attached waveguides (termed the “unequal case”) and without the waveguides attached (termed the “equal case”). The feedhorn radiation is modeled as ideal 2-D Gaussian in shape (and zero power in the crosspolar pattern) with an 18 dB taper from the center of the dish to its outside edge. Shown in Fig. 2 are several ϕ cuts (i.e., azimuth) of the antenna patterns for transmit horizontal polarization: black is a 0^o copolar; magenta is 45^o copolar; blue is 0^o crosspolar; red is 45^o crosspolar. For a center-fed parabolic reflector topology, the maximum crosspolar signal occurs in the $\pm 45^o$ ϕ planes. Examining the crosspolar 45^o cut (red line) at 0^o on the horizontal axis (θ), it is seen that the crosspolar minimum is less than -5 dB while the copolar maximum is about 46 dB. The crosspolar signal remains very low across the copolar main lobe. The conclusion is that the crosspolar coupling is very low relative to the copolar patterns so that an ICPR of -31 dB can not be accounted for (i.e., it would be much lower for the shown cuts). Thus, the feedhorn of S-Pol must be the cause of this high ICPR figure. Additionally, the OMT (orthomode transducer) of the S-Pol feedhorn is physically very short and thus the extraneous electric field modes can not be suppressed sufficiently below the fundamental TE11 mode (Olver and Clarricoats 1994). Thus, to improve the ICPR figure of S-Pol, a new feedhorn (with the OMT) is required. According to the manufacturer, Custom Microwave of Longmont, CO, S-Pol’s new feedhorn has better than 40 dB isolation in all ϕ planes.

Next the theoretical 3-D antenna patterns of the new feedhorn (both copolar and crosspolar) are used in the GRASP model to predict the S-Pol antenna patterns. Shown in the top panel of Fig. 3 is the H copolar power pattern for the unequal struts case. The non symmetric pattern is caused by the support strut blockage.

Of particular interest are the crosspolar patterns f_{hv} and f_{vh}, both power and phase, and how they affect ICPR calculations. For reference, we first show the crosspolar phase pattern for a perfect reflector, no strut blockage and a perfect Gaussian feedhorn pattern in the bottom panel of Fig. 3. The radius of the pattern is 3^o. For a constant radius the phase is constant but jumps 180^o at the quadrant boarders. Along a line of constant ϕ, the phase keeps decreasing.

Figure 4 shows the cropsspolar power antenna patterns: top left, $|f_{hv}|^2$, for equal struts; top right, $|f_{vh}|^2$, for equal struts; bottom left, $|f_{hv}|^2$, for unequal struts; and bottom right $|f_{vh}|^2$, for unequal struts. Ideally these patterns would be symmetric about the H, V and $\pm 45^o$ planes. The strut blockage (and the distorted dish) causes the patterns to lose symmetry. It can also be seen that the unequal strut case (bottom two panels) have increased power compare to the corresponding equal strut patterns in the top two panels. Figure 5 show the crosspolar phase patterns corresponding to the power patterns shown in Fig. 4. The phase patterns are now quite complicated as compared to the “ideal” case of Fig. 3, bottom panel. The phases of unequal strut case are seen to be more variable than that seen in the equal strut plots.

4.1. *Modeled ICPR*

To our knowledge, up to this point in the literature, ICPR_{ub}, instead of ICPR, has been calculated using only antenna power patterns since the crosspolar phase patterns have not been available. With the GRASP modeled complex antenna patterns, ICPR can be calculated using Eq.(5) and these calculation can be compared to ICPRub of Eq.(6). These numbers are given in the table below for both the unequal and equal strut cases.

	ICPR$_{ub}$ (dB)	ICPR (dB)
Eq. Struts	-36.5	-41.2
Uneq. Struts	-30.1	-34.4

Thus, the expected ICPR of the S-Pol antenna with the new feedhorn is -34.4 dB. However, if the support struts can be made to be equal dimensionally, then the ICPR improves to -41.2 dB.

The ICPR and ICPR$_{ub}$ differ by around 5 dB in both cases. From Eq.(5), it is obvious that there is a reduction in the magnitude of the numerator term $f_{hh}f_{vh} + f_{vv}f_{hv}$ due to the inclusion of the pattern phases. For minimization of Eq.(5) to occur, ideally $\arg\{f_{hh}f_{vh}\} = \arg\{f_{vv}f_{hv}\} + \pi$, at each point in space. Figure 6 shows $\arg\{f_{hh}f_{vh}\} - \arg\{f_{vv}f_{hv}\}$ patterns for equal struts (top panel) and unequal struts (bottom panel). Note that the radius for these plots is 2^o. As can be seen, the phase of the unequal strut case in the lower two quadrants for a radius$< 1^o$ is significantly father away from 180^o as compare to the equal strut case. This is why ICRP<ICPR$_{ub}$. For completeness the corresponding $|f_{hh}f_{vh} + f_{vv}f_{hv}|^2$ antenna patterns are shown in Fig. 7. Note the patterns have not been normalized by the copolar power. As can be seen, there is a significant increase in $|f_{hh}f_{vh} + f_{vv}f_{hv}|^2$ for the unequal strut case.

5. $\mathbf{Z_{dr}}$ AND ANTENNA ERRORS

Beginning with Eq.(3), simultaneous transmit H and V mode (SHV) differential reflectivity (Z_{dr}^{SHV}) is

$$10\log_{10}\frac{|V_v|^2}{|V_h|^2} = Z_{dr}^{SHV} = 10\log_{10}\Big[\frac{\sum_i [f_{hh}^2 + f_{hv}^2 + f_{hh}f_{vh} + f_{vv}f_{hv}]|^2 d\Omega}{\sum_i |f_{hh}f_{vh} + f_{vv}f_{hv} + f_{vv}^2 + f_{vh}^2|^2 d\Omega}\Big] \qquad (7)$$

where $E_H = E_V = 1$ in Eq.(3) and $d\Omega = sin\theta\delta\theta\delta\phi$. As can be seen the first order errors in Z_{dr}^{SHV}, namely $f_{hh}f_{vh} + f_{vv}f_{hv}$, are identical to the error term in the numerator of ICPR. Thus, in general, reducing ICPR by good antenna design also reduces biases in Z_{dr}^{SHV}. See Hubbert et al. (2010a,b) for details.

6. SUMMARY

Over the past few years modeling software for parabolic reflector antennas, such as GRASP, has improved so that accurate prediction of the *complex* antenna patterns can be calculated. The true (measured) shape of the reflector, support strut blockage and feedhorn patterns can all be included. This was done for S-Pol's antenna as part of a project to improve antenna performance. Modeling studies showed that the feedhorn (including OMT) was the principal cause of S-Pol's -31 dB ICPR estimated from measurements in light rain. Modeled antenna patterns for a newly designed feedhorn were then used in the GRASP model. The model indicated that the ICPR should improve to -34.4 dB. The model also demonstrated the importance of symmetry on the antenna design. Currently, two of S-Pol's support struts carry the H and V waveguides up to the feedhorn (see Fig. 1). The model indicates that if the supports struts could be made physically "equal" in their outside dimensions, ICPR could be reduced to better that -40 dB. To accomplish this, the wave guide could be placed inside the support struts. NCAR will mount and test the new feedhorn on S-Pol late Summer 2012.

Acknowledgment

This research was supported in part by the ROC (Radar Operations Center) of Norman OK. Both the CSU-CHILL and NCAR S-Pol radars are supported by the National Science Foundation. Any opinions, findings and conclusions or recommendations expressed in this publication are those of the authors and do not necessarily reflect the views of the National Science Foundation.

References

Chandrasekar, V. and R. Keeler, 1993: Antenna pattern ananlysis and measurements for multiparameter radars. *J. Atmos. Oceanic Technol.*, **10**, 674–683.

Hubbert, J., S. Ellis, M. Dixon, and G. Meymaris, 2010a: Modeling, error analysis and evaluation of dual polarization variables obtained from simultaneous horizontal and vertical polarization transmit radar. Part I: Modeling and antenna errors. *J. Atmos. Oceanic Technol.*, **27**, 1583–1598.

— 2010b: Modeling, error analysis and evaluation of dual polarization variables obtained from simultaneous horizontal and vertical polarization transmit radar. Part II: Experimental data. *J. Atmos. Oceanic Technol.*, **27**, 1599–1607.

Olver, A. and P. Clarricoats, 1994: *Microwave Horns and Feeds*. Institution of Electrical Engineers, London, UK, 494 pp.

Wang, Y. and V. Chandrasekar, 2006: Polarization isolation requirements for linear dual-polarization weather

radar in simultaneous transmission mode of operation.
IEEE Trans. Geosc. and Remote Sen., **44**, 2019–2028.

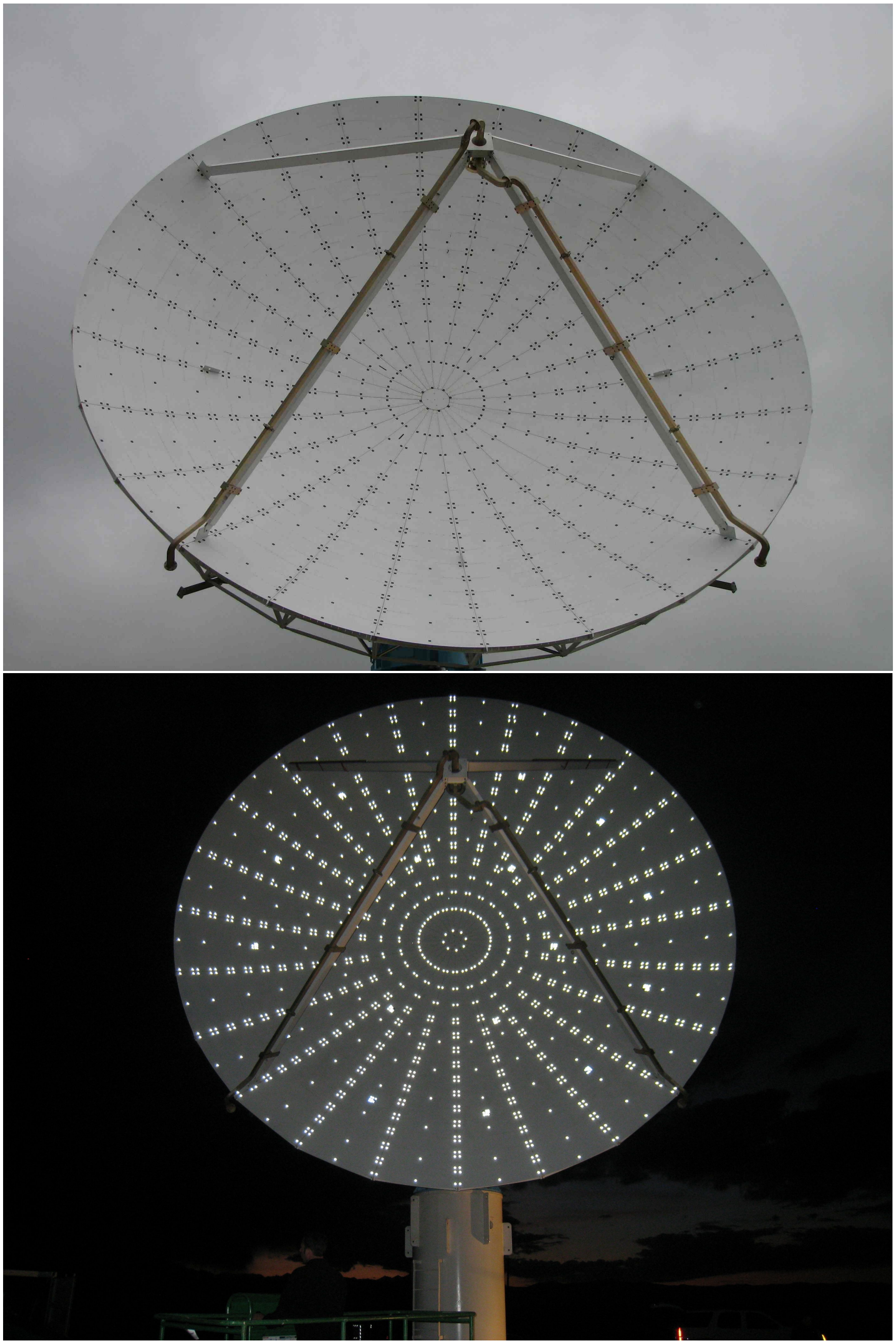

Figure 1: *S-Pol antenna. Top panel; optical patches are seen as darker spots. Bottom panel; a flash camera picture at night.*

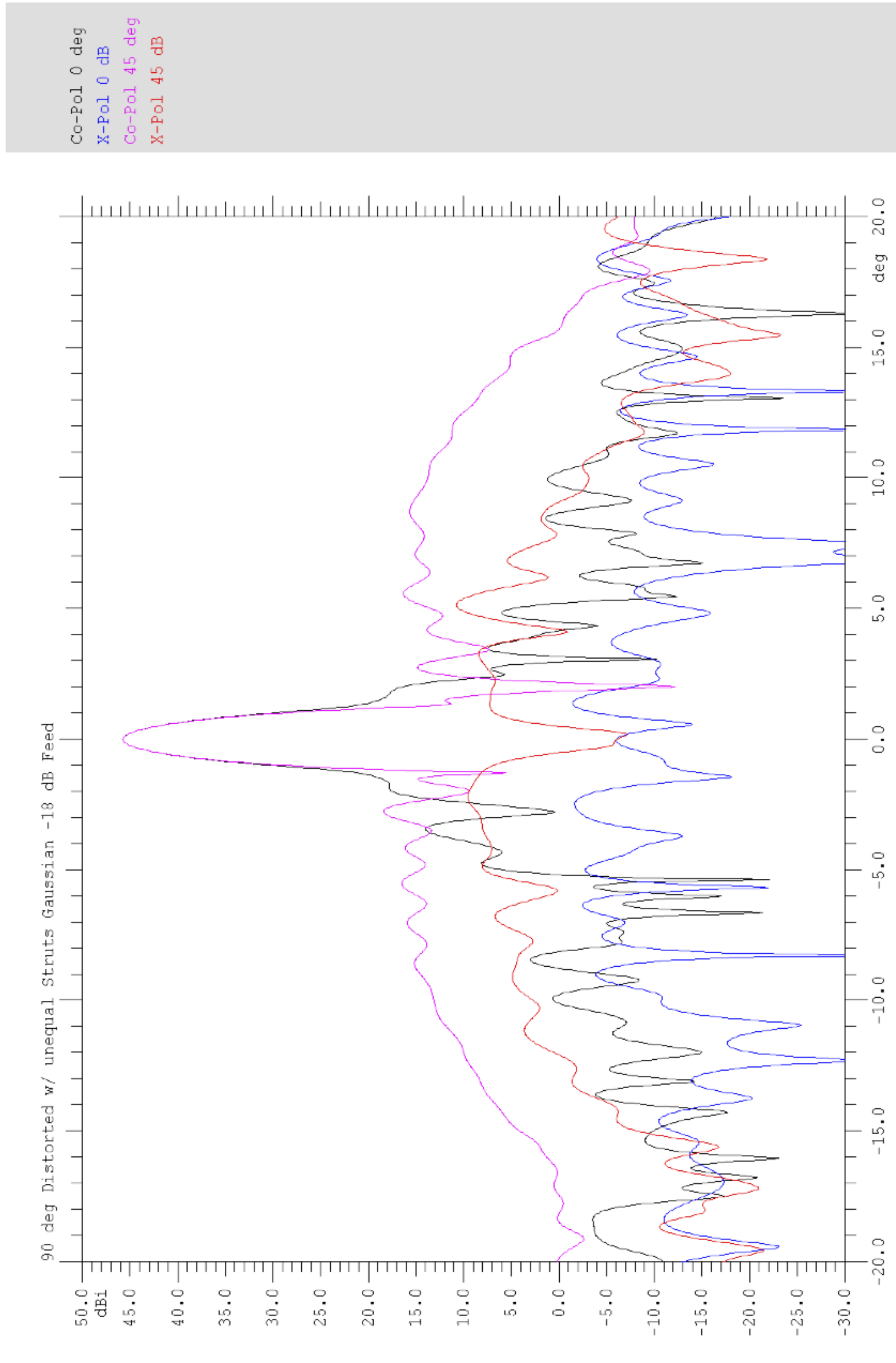

Distorted with Un-equal Struts

Figure 2: *S-Pol antenna pattern ϕ (azimuth) cuts. Modeled data.*

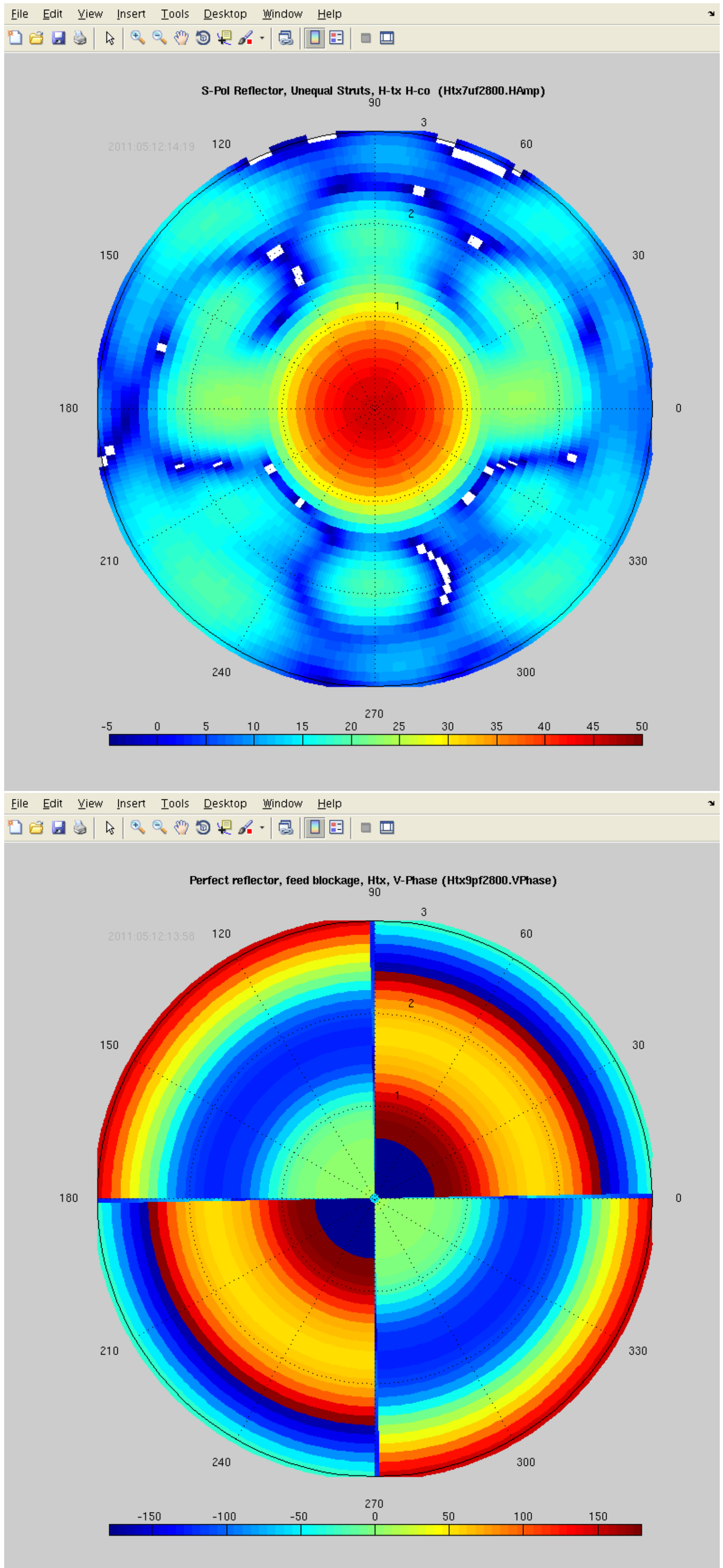

Figure 3: *Modeled S-Pol's antenna patterns: top panel, H coplar power pattern (dBi); bottom panel, ideal crosspolar phase pattern. The radius is 3^o for both panels.*

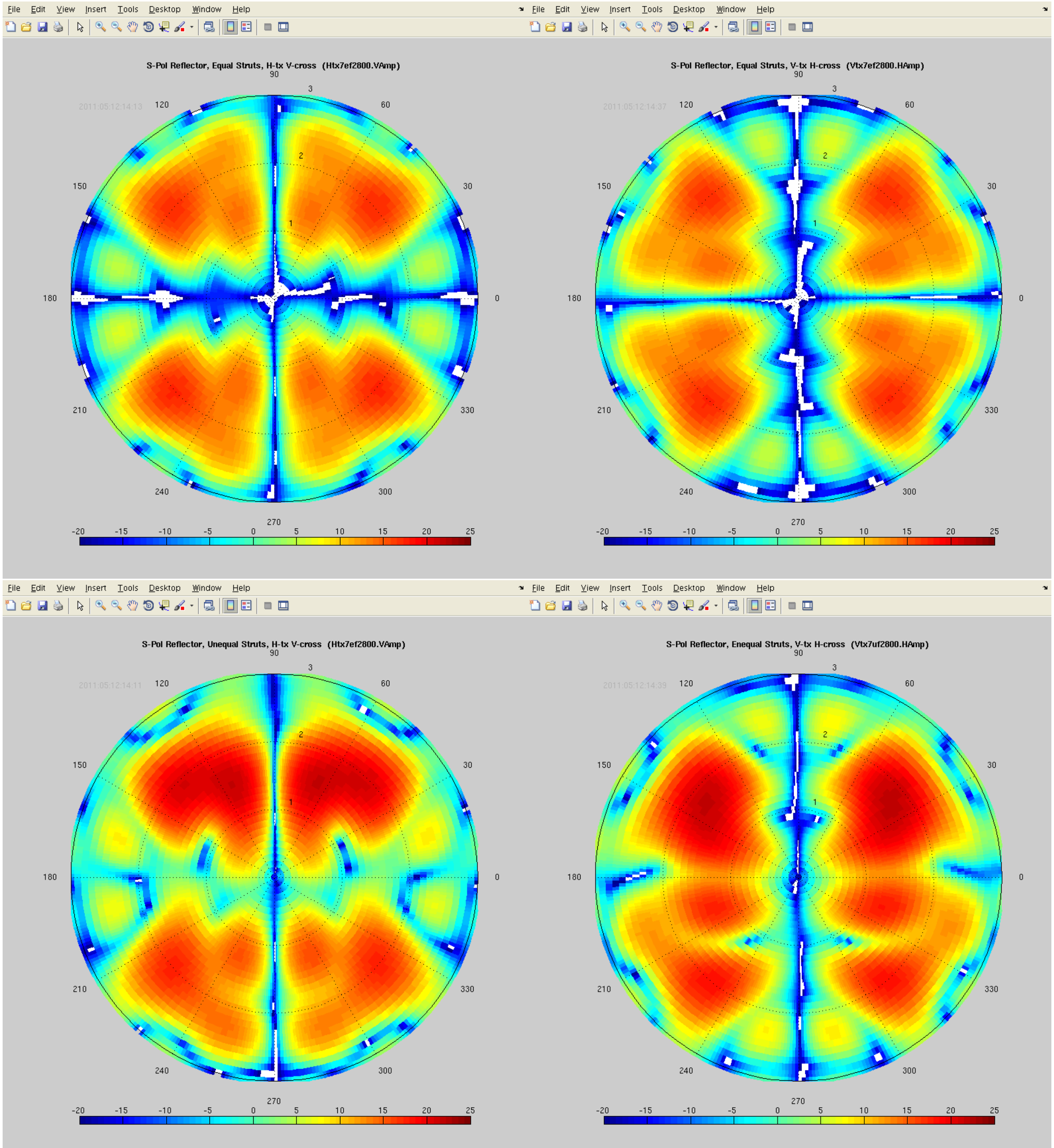

Figure 4: *Moddeled S-Pol cropsspolar power antenna patterns (dBi): top left, $|f_{hv}|^2$, equal struts; top right, $|f_{vh}|^2$, equal struts; bottom left, $|f_{hv}|^2$, unequal struts; bottom right $|f_{vh}|^2$, unequal struts. The radius is 3^o for all panels.*

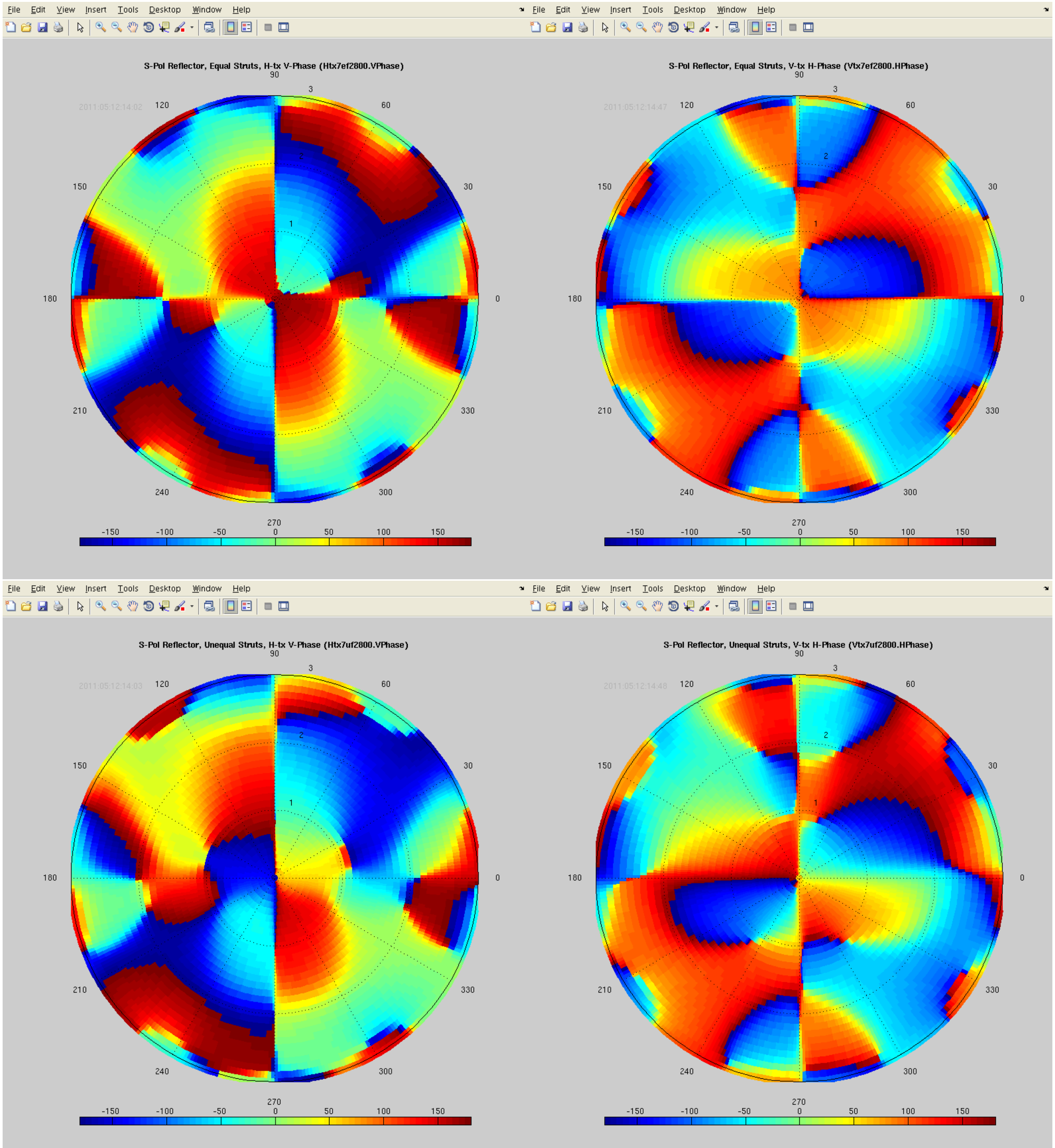

Figure 5: *Modeled S-Pol crosspolar phase antenna patterns corresponding to Fig. 4.*

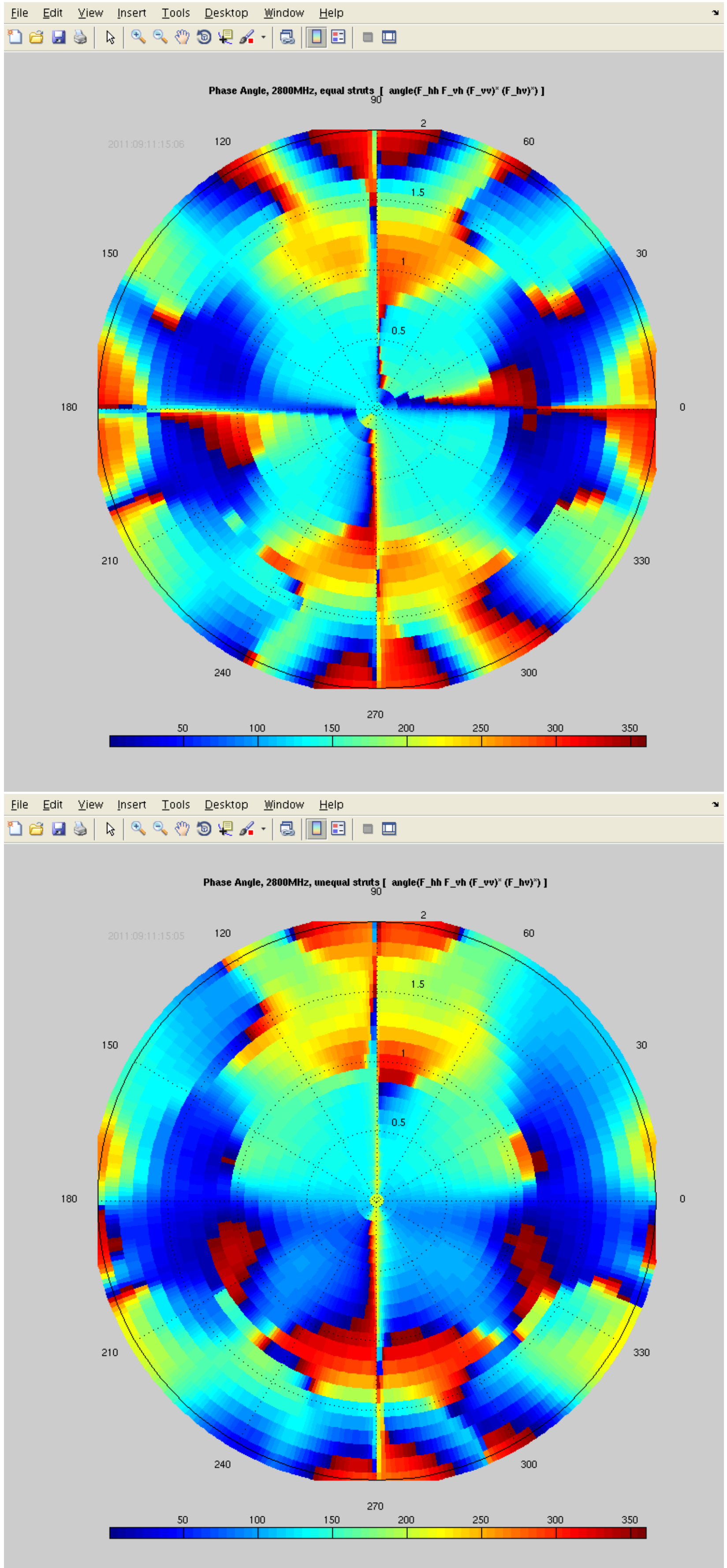

Figure 6: *The modeled S-Pol phase antenna pattern for* $\arg\{f_{hh}f_{vh}\} - \arg\{f_{vv}f_{hv}\}$. *The radius is* 2^o.

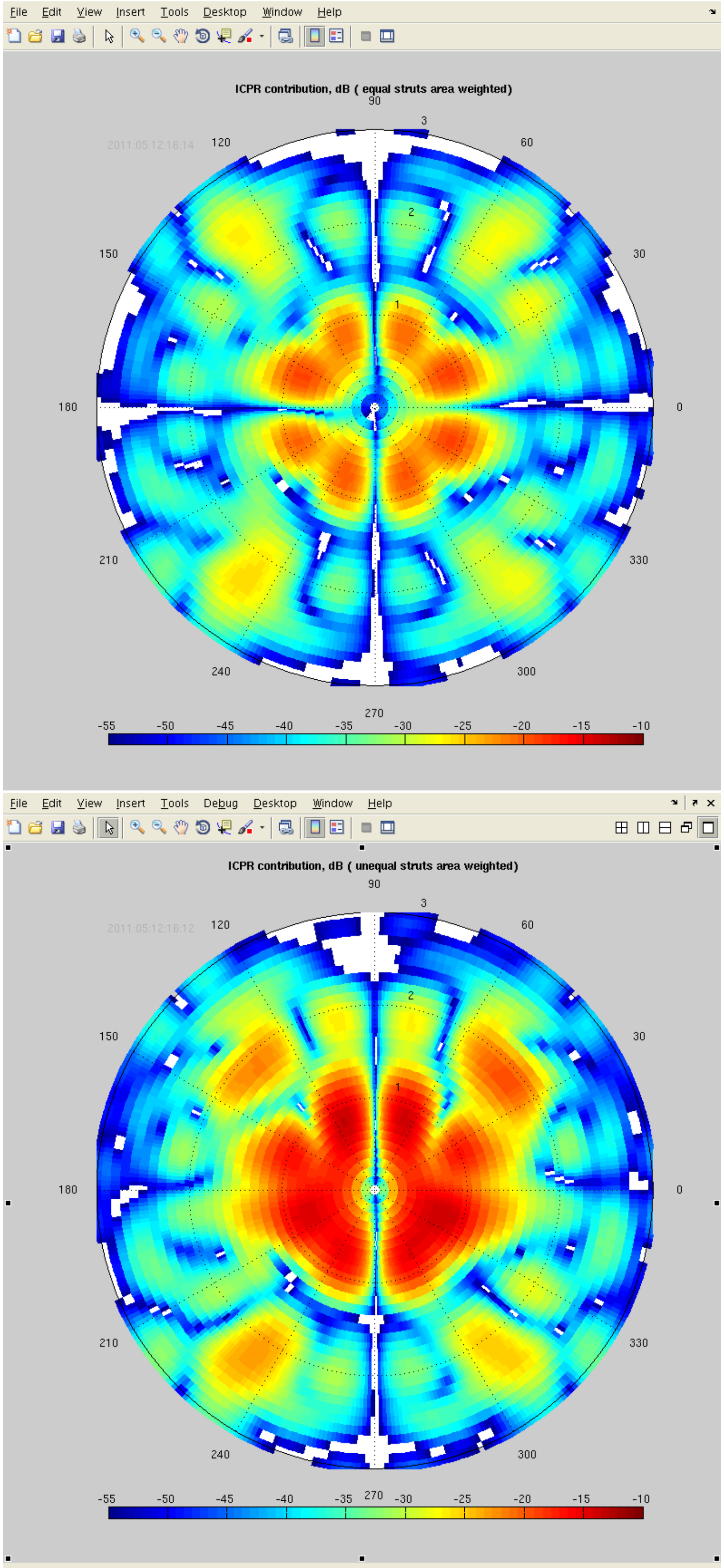

Figure 7: *Modeled S-Pol antenna patterns (dB) of* $|f_{hh}f_{vh} + f_{vv}f_{hv}|^2$ *corresponding to Fig. 5. Note that the radius here is* 3^o *while in Fig. 6 the radius is* 2^o*.*